ALUMINIUM PREATREATMENT AND THE PROPERTIES OF ADHESIVELY BONDED JOINTS

Irene Jansen[+]*, Frank Simon[++], Rüdiger Häßler[++], Horst Kleinert[+]

[+] Dresden University of Technology, Institute of Production Technology, 01062 Dresden, Germany, e-mail: jansen@mciron.mw.tu-dresden.de

[++] Institute of Polymer Research Dresden e.V., Dresden, Hohe Str. 6, 01069 Dresden, Germany; e-mail: rhaesz@ipfdd.de

SUMMERY: The influence of metal pretreating on the properties of adhesively bonded joints was investigated. AlMg3 and several pre-treatment methods were used.

The pre-treated surfaces and the joints were characterized using: SEM/EDX, XPS, EIS, surface tension, DMA, μTA and the determination of mechanical parameters.

The highest bond strengths were obtained using anodic oxidation in phosphoric acid as the pre-treatment method.

Introduction

It is known that the aluminium oxide/hydroxide, present at aluminium surfaces, has a significant influence on the adhesion behaviour of adhesives[1]. The reason for this is the formation of an interphase between the metal oxide surface and the interacting polymeric adhesive. In contrast to the often discussed interface, which contains only the directly interacting layers of the two contacting phases, an interface has third dimension. The third dimension is characterized by a graduated structure formation and properties different from those of the bulk phase. In other words, the polymers used as adhesives can be considered as an inhomogeneous polymer layer[2] with a depth-depending profile of molecular ordering, physical and microscopic mechanical properties. It is very simple to understand that the graduated properties determine the macroscopic properties of a joint. Nevertheless, the

 CCC 1022-1360/00/$ 17.50+.50/0

formation of an interphase, its presence and influence of the macroscopic mechanical stability of a joint is not generally accepted.

During the last few years a lot of work has been done to visualize such interphases and study their property changes in dependence on the distance from the metal oxide surface. Surface sensitive methods, like e.g. atomic force microscopy (AFM)[3,4], X-ray photoelectron spectroscopy (XPS)[5], FT-IR spectroscopy[6], ellipsometry[7] or scanning electron microscopy (REM)[8] with information depths of a few nanometers were used to characterize the polymer layers on metal oxide surfaces. Other authors[9] determined mechanical parameters of joints made from aluminium sheets and more or less suitable adhesives, and applied these parameters for modelling by finite element analyses (FEA) to describe the influence of the pre-treated metal surface on adhesion strength and polymer structures.

An important result of all these studies was that the interface properties of a certain polymer and their lateral changes are strongly influenced by the kind of substrate material. This work is a contribution for a better understanding of the aluminium oxide/hydroxide surface structure and its influence on an adhering polymer layer in a thickness of several micrometers. The results are not only important for the understanding of fundamental processes in adhesion science; they can also be used to optimize the chemical and mechanical properties of adhesively bonded joints and better their reliability and life spans.

Experimental

Materials:

Sheets of the aluminium/magnesium alloy AlMg3, with a thickness of 1.5 mm, were used as substrate materials. The AlMg3 samples were pre-treated, using different methods:

1. Anodic oxidation in phosphoric acid at 15 V and 0.3 A/dm^2 (PAA).
2. Anodic oxidation in sulphuric acid at 15 V and 1.5 A/dm^2 (SAA).
3. Grit blasting using corundum particles K 24, particle diameter of 0,7 – 0,85 mm.
4. Pickling in chromo sulphuric acid (CSA).
5. Ultrasonic degreasing with acetone.
6. Etching with NaOH.

The adhering polymer was a resin system from diglycidylether of bisphenol A and F (Epilox T 19-34 from Leuna, Germany) crosslinked with the cyclo-aliphatic diamine isophorone diamine (Epilox H10-31 from Leuna, Germany).

Methods for characterization:

Scanning Electron Microscopy (SEM/EDX):

Electron micrographs were obtained with a DSM 982 GEMINI (Zeiss, Germany) at 10keV. Preatreated surfaces were steamed with gold. For the preparation of the traverse section joints were embedded in epoxide resin, polished and steamed with gold. EDX-investigations were made with a Voyager (Noran Instruments) until 3 000 counts. The quantitative evaluation followed according to the Proza correction.

X-ray Photoelectron Spectroscopy (XPS):

XPS was carried out using an ESCAlab 220i spectrometer (Vacuum Generators, UK) equipped with a non-monochromatized Mg K_α X-ray source. The kinetic energy of photoelectrons was determined using a hemispherical analyzer with a constant pass energy of 80 eV for survey spectra and 25 eV for high-resolution spectra. All spectra were referenced to the hydrocarbon reference peak C 1s at binding energy BE = 285.00 eV.

In the case of smooth samples the take-off angles Θ were 0°, 45° and 60°. Here, the take-off angle is defined as the angle between the sample's surface normal and the electronoptical axis of the spectrometer. Hence, the maximum information depth of XPS is not more than 10 nm.

Quantitative elemental compositions were determined from peak areas after using Wagner's sensitivity factors and the spectrometer transmission function.

The high-resolved spectra were decomposed by means of the VG ECLIPSE routines. Free parameters of component peaks were their binding energy, height, full width at half maximum and the Gaussian-Lorentzian ratio.

Electrochemical Impedance Spectroscopy (EIS):

The Impedance spectrograms were obtained with an IM 6 (Zahner electric) by a potential of 900 mV. Density/potential measurements were made after ageing of the pretreated samples in seawater.

Contact angle measurements:

Contact angle were measured by the sessile drop technique with a G 40 (Krüss GmbH) and water and methylene iodide as test liquids or by the Wilhelmy balance technique with a tensiometer K 121 (Krüss GmbH) and water as test liquid.

Dynamic Mechanical Analysis (DMA):

Dynamic Mechanical Analysises were obtained by a DMA 981 (Du Pont) under nitrogen atmosphere. The heating rate was 3 K/min and the temperature range was between -40 °C and +300 °C.

Micro thermal analysis:

The investigations were carried out with a μTA™ 2990 system (TA Instruments). A polyamide standard was used for temperature calibration. The tip temperature during the scan was 50 °C. The heating rate of the local thermal analysis was 10 K/sec.

Shear tension test:

The tests were made with a shear tension machine AGS-G (Shimadzu). The maximal tensile stress is 10 kN.

Results and Discussions

The pretreated surfaces were characterized using SEM. Anodic oxidations in phosphoric acid as well as sulphuric acid led to cellular structures of the aluminium oxide surface layers (fig. 1).

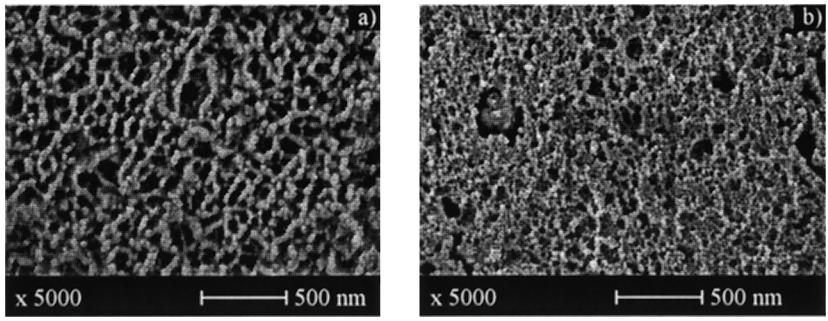

Fig. 1: SEM images of AlMg3 surfaces after their anodic oxidation in phosphoric acid (a) and sulphuric acid (b), respectively.

To determine the thickness of the anodically oxidized aluminium layer EDX linescans of oxygen and aluminium were recorded (Fig. 2). Oxygen is a labelling element only for the aluminium surface covering oxide layer, while aluminium can be observed from the oxidized top layer as well as the bulk substrate material. According to the EDX measurements the thickness of the oxide layer was 1 μm (anodic oxidation in phosphoric acid, fig. 2a) or 8 μm (anodic oxidation in phosphoric acid fig. 2b).

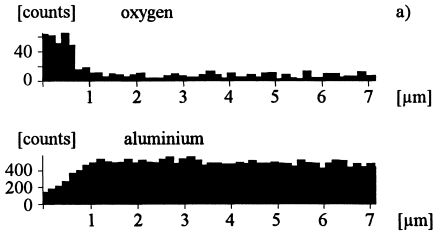

Fig. 2a: EDX linescans of oxygen and aluminium recorded from an anodically oxidized aluminium sheet (phosphoric acid)

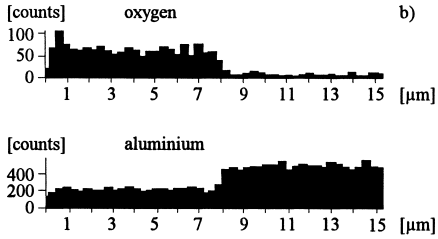

Fig. 2b: EDX linescans of oxygen and aluminium recorded from an anodically oxidized aluminium sheet (sulphuric acid)

XPS was used to investigate the elemental surface composition. Besides, the qualitative and quantitative determination of all key elements (aluminium, oxygen and carbon), the knowledge of the mean free path of the photoelectrons λ allows the evaluation of the surface layer thickness d. The relative areas of the peak due to oxide with respect to metal are given as[10]

$$\frac{I_{Al2p}(\underline{Al}_2O_3)}{I_{Al2p}(\underline{Al}_x)} = \frac{1-\exp[-d/(\cos\Theta\cdot\lambda)]}{\exp[-d/(\cos\Theta\cdot\lambda)]} \qquad (1)$$

Where $I_x(Y)$ is the normalized peak area of the component peak x of the species Y, and Θ the take-off angle defined above. For photoelectrons appearing from the Al 2p level λ is approximately 13 ± 2 Å[10,11]. Eq. 1 shows that it is not necessary to carry out angle-resolved XPS experiments to determine d. However, with increasing Θ the surface sensitivity of the method is increased. An important problem for the interpretation of the XPS results concerning their depth information is the surface roughness, which increases with increased sample treatment time. However, Slomkowski et al.[12] showed impressively that an angle dependence of the photoelectron intensity could also be observed on extremely rough surfaces.

Fig. 3 shows typical highly-resolved Al 2p spectra of pickled alumina surfaces. The spectra recorded at different take-off angles show two component peaks indicating the two expected chemical states of alumina. Component peak A found at a binding energy of XXX eV appears from the metallic aluminium species, while component peak B corresponds with Al–O bonds. The high shift in the binding energy indicates a rather Lewis acidic aluminium oxide/hydroxide species on the sample's surface[13].

It can be clearly seen in fig. 3 that the measured intensities of the two component peaks depend on the take-off angle. The dependence agrees with the expected enhanced surface sensitivity of the method. From the measured component peak intensities, depending on the take-off angles, we calculated the layer thickness of the oxide layer on the pickled aluminium surface according to eq. 1. In all cases we found layer thickness independent on the take-off angles. That is not surprising, because the take-off angle is an experimental parameter selected only for XPS analysis, and is not connected with the layer thickness created during the pickling procedure. Furthermore, it is well known that the oxide layer fully covers the aluminium surface. Hence, the assumption of the simple overlay model (eq. 1) is fulfilled. Nevertheless, we treated all XPS data with the model of Opila et al.[14] assuming surface layers do not fully cover the substrate. Here, we found the same values of layer thickness and degrees of substrate coverage of ca. 0.9 indicating a fully coated substrate material.

All these results show that angle-dependent measurements can be applied to enhance the surface sensitivity of the XPS method.

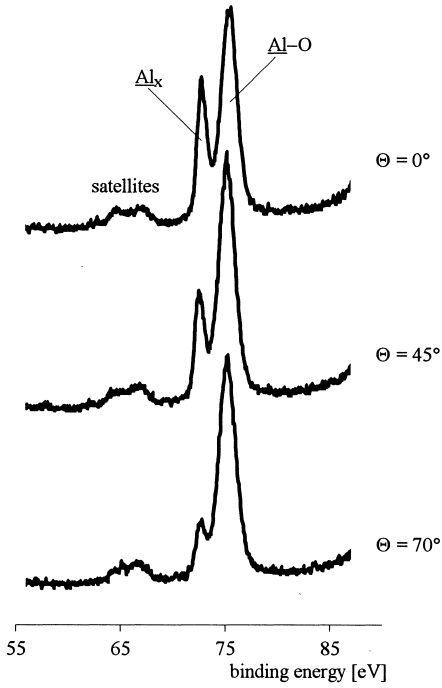

Fig. 3: High-resolved Al 2p spectra of pickled alumina surfaces recorded after storage in air for 2000 s for three different take-off angles Θ. Spectra show two component peaks of different intensity (for all spectra the area of the Al–O component peak was the same). The component peak Al_x indicates the presence of metallic aluminium, while Al–O appears from the oxidized surface layer.

We used the angle-resolved XPS measurements described above to investigate the time-dependence of the formation of a thin oxide layer and structural changes therein after a pickling pre-treatment (fig. 4).

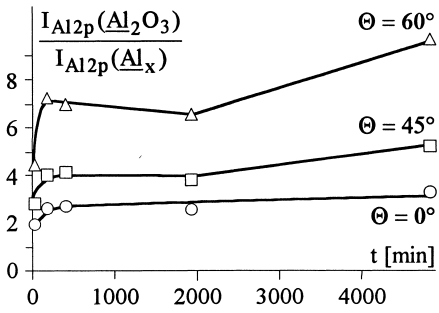

Fig. 4a: Intensity ratios of the Al 2p component peaks in dependence on the time after the pickling pre-treatment (t) of aluminium sheet.

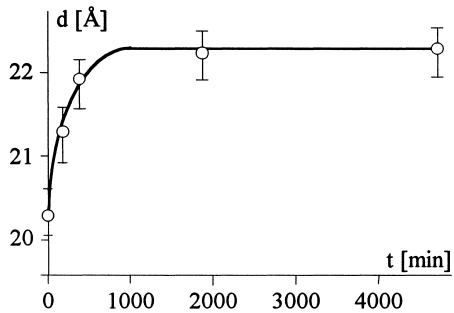

Fig. 4b: Thickness d of the oxide layer on alumina in dependence on the time after the pickling pre-treatment (t) determined according to eq. 1. Bars indicating the scattering of d values at different take-off angles.

Fig. 4a shows that the relative amount of the oxidized aluminium species increases with the time after the surface treatment. Similarly, the oxide layer thickness is also increased (fig. 4b). After ca. 1000 minutes a constant thickness d of ca. 22 Å was obtained. That value agrees well with d values determined for annealed and hot rolled alumina foils[10]. The constant layer thickness is not an indicator for an equilibrium in surface layer formation. Fig. 4a demonstrates clearly that structure changing processes take place a long time after reaching a constant oxide layer thickness. It can be assumed that, during the storage in air, water and additional amounts of oxygen are introduced to the top of the surface layer. That process may be interpreted as a compacting of the oxide/hydroxide surface layer.

The Bode plots in fig. 5 were obtained using EIS. Comparing the differently pre-treated aluminium sheets, anodically oxidized aluminium shows the highest impedance values. The lowest values were found for grit blasted aluminium. The oxide layer has two functions: protection of aluminium against corrosion and a good adhesion ground for the polymer. In this point, anodically oxidized aluminium is well suitable for the formation of a durable joint.

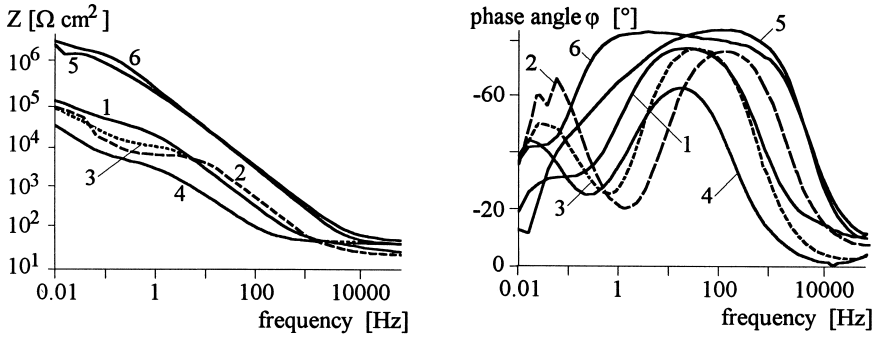

Fig. 5: Bode plots obtained from EIS measurements of the differently pre-treated aluminium sheets (1 degreasing, 2 polish, 3 pickling, 4 grit blasting, 5 anodically oxidized in H_3PO_4, 6 anodically oxidized in H_2SO_4)

After ageing of the samples in seawater the aluminium, which was anodised in sulphuric acid, was found to have the greatest stability. This was shown from the current density/potential measurements (fig. 6).

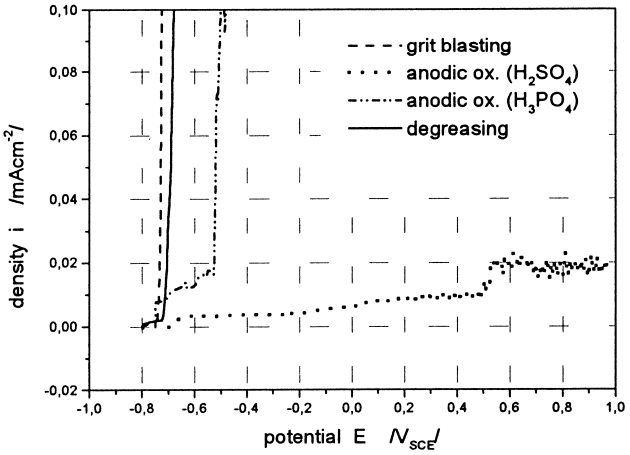

Fig. 6: Density/potential measurements after ageing of pretreated AlMg3 in seawater.

Static advancing and receding contact angles were measured on the surfaces of the substrates by the sessile drop technique using a conventional goniometer technique (fig. 7). Calculations of the solid surface tension from the contact angle values were made with the method of Owens, Wendt, Rabel and Kaelble. Dynamic advancing and receding contact angles were measured using the Wilhelmy balance technique (fig.8). The determination of the advancing contact angle showed lower values and, therefore, increased solid surface tension when the surface was pretreated. In this case the wetting behaviour of the adhesive was better.

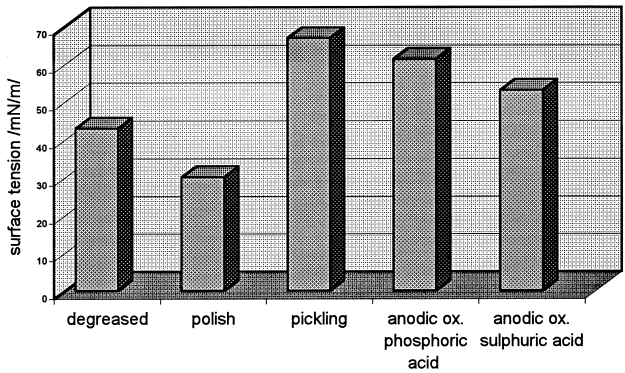

Fig. 7: Dependence of the surface tension on the pretreatment (sessile drop technique).

The difference between the advancing contact angle and the receding contact angle (hysteresis) was small in the case of the anodic oxidation pre-treatment of the metal. This means that relatively homogeneous layers were formed with a low roughness. Measurements of the roughness confirmed this.

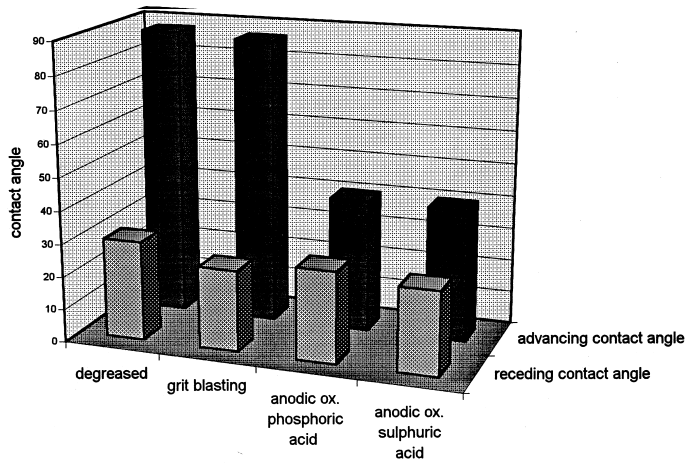

Fig. 8: Dependence of the contact angles on the pretreatment (Wilhelmy balance technique).

By the Dynamical Mechanical Analysis (DMA) we found several different glass transition temperatures of the joints dependent on the pretreatment up to an adhesive layer thickness of 0,08 mm (fig. 9). At greater thicknesses the surface influence on the glass transition temperature of the joint decreased and the bulk properties of the epoxy resin dominated. In this case we found similar glass transition temperatures for several pretreatments[15].

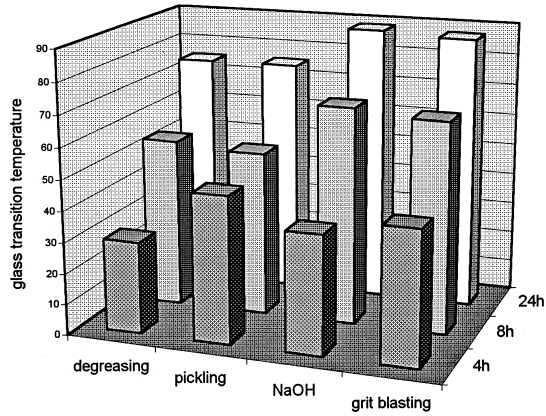

Fig. 9: The dependence of the glass transition temperatures of the joints on the pretreatment of the aluminium and the curing time. The measurements were made with DMA.

The formation of adhesive interphases with distinct properties has already been proven in AFM studies, including a mechanical characterisation by Force-Modulation-Mode AFM (AFM-FMM). The AFM measurements showed that the elasticity close to the surface is smaller than in the bulk. The layer has the same elasticity when the surfaces are only degreased. The FT-IR spectra we obtained from the phases close to the aluminium surfaces and in the bulk were in accordance with this[16].

The novel technique of µTA™, a combined method of AFM and Thermal Analysis, offers the opportunity to characterise the thermal properties of the interphase area in microscopic dimensions[17, 18]. You can display the topography of the scan area between the polymer and the substrate of a composite. The topography in this case does not allow an unambiguous interpretation of the image. In contrast the thermal conductivity image easily reveals the position of the interface: the higher thermal conductivity of the metal results in bright colours (left in fig. 10) and is distinguished from the areas of poorer conductivity where resin is located, shown in darker colours (right in fig. 10). The conductivity decreases with distance from the metal in the polymer. The thermal conductivity of a sample is generally a function of its density and for crosslinked samples it is thus a function of the crosslinking density. Highly crosslinked material shows a high thermal conductivity. Thus, these results agree well with the observations made with AFM in force modulation mode.

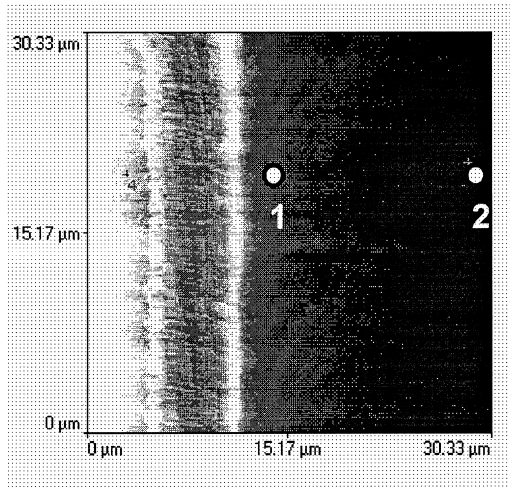

Fig. 10: Thermal conductivity image of the interphase area in a composite.

Generally the cross-linking density of a polymer is characterised by its glass transition temperature. With μTA it is possible to measure these temperatures locally at selected positions on the sample surface. The glass transition causes a softening of the surface and thus the temperature can be well defined by monitoring changes in the μTMA signal during an LTA experiment. As the surface softens the probing tip 'sinks' into the surface, resulting in a deviation of the signal from the expansion slope of the initially hard material.

The thermal conductivity image of the cross-section of an epoxy resin/aluminium interface area is shown in fig. 10[19]. Prior to processing the aluminium sheet was treated by an anodic oxidation in phosphorous acid. This treatment results in an oxide layer at the surface of the sheet. Indeed in the image a more than 5 μm wide area can be recognized on the right-hand side of the bulk metal. The polymer is represented by dark grey-values, indicating a drastically reduced thermal conductivity. Close to the interface between polymer and oxide layer (labelled '1' in fig. 10) the conductivity values of the polymer are increased compared with those of the bulk polymer (labelled '2' in fig. 10).

A more quantitative analysis of the interface is possible using the local thermal analysis (LTA) capabilities of μTA. The μTMA curves obtained on bulk metal or at the oxide layer show only thermal expansion without any transition. The slope of the μTMA signal measured at the oxide layer is significantly reduced due the lower thermal conductivity and the lower expansion coefficient of this layer. The μTMA curve obtained at the polymer in the immediate vicinity of the interface (fig. 10, point 1) shows a significant softening transition around 138°C. Furthermore, the temperature of the softening transition in the bulk decreases to values of 118 °C (fig. 10, point 2). This value agrees well the results of T_g measured by DSC and DMA on pure epoxy samples.

Thus it may be concluded that the pretreated surface has a significant impact on the cross-linking of the epoxy resin. The question remains whether the oxide layer plays an immediate role in the cross-linking of the polymer, as suggested in the literature.

Fig. 11 shows the influence of different substrate pretreatments on the glass transitions in the epoxy resin both in the bulkphase and near the substrate surface.

The local thermal analysis at differing distances from the substrate surface allows a profile to be made of the network density of the epoxy resin in dependence on the substrate surface.

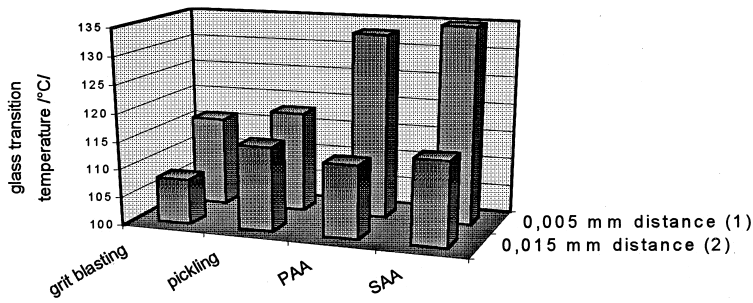

Fig. 11: Influence of pre-treatment on the glass transition temperature Tg of the epoxy resin at different distances from the substrate surface.

Further methods were carried out for the characterization including determination of the mechanical parameters (shear tension test) (fig. 12). The best values for the lap shear strength were found for joints formed from anodic oxidised aluminium (phosphoric acid).

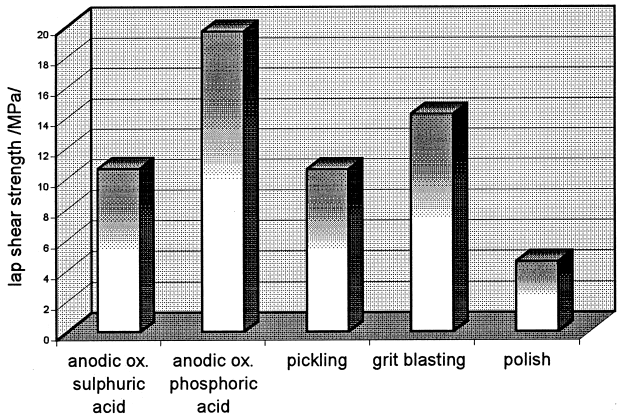

Fig. 12: Shear tension test.

Conclusion

The influence of different adhesion pretreatments on the network structure of epoxy resin was investigated using several methods. AFM, FT-IR and especially μTA were useful for characterizing the structure at different distances from the pretreated surface.
From the results of the shear tension test the best pretreatment method is anodic oxidation in phosphoric acid.

Acknowledgements

The authors would like to thank Dr. Nocke (Institute of Material Science, TU Dresden) for the Electrochemical Impedance Spectroscopy measurements.
Financial support from Deutsche Forschungsgemeinschaft (DFG, SFB 287) is gratefully acknowledged.

References

[1] R. G. Schmidt *Adv. Polym. Sci.* **1986**, *75*, 33
[2] T. Drzal *Adv. Polym. Sci.* **1986**, *75*, 1
[3] T. Gesang, R. Höper, W. Possart, O.-D. Hennemann *Adhäsion kleben & dichten* **1995**, *39*, 27
[4] T. Gesang, R. Höper, W. Possart, O.-D. Hennemann *Adhäsion kleben & dichten* **1995**, *39*, 40
[5] W. Possart *J. Adhesion* **1995**, *48*, 25
[6] W. Possart, a. Hartwich, O.-D. Hennemann *Adhäsion kleben & dichten* **1995**, *39*, 25
[7] D. Fanter, W. Possart, O.-D. Hennemann *Adhäsion kleben & dichten* **1995**, *39*, 30
[8] O. Hahn, G. Kötting *Kunststoffe* **1984**, *74*, 238
[9] O. Klapp, K. Reiling, M. Schlimmer *Adhäsion kleben & dichten* **1998**, *42*, 33
[10] D.T. Clark, K.C. Tripathi *Nature Phys Sci* **1973**, *241*, 162
[11] D. Briggs, M.P. Seah *Practical Surface Analysis. Volume 1 – Auger and X-ray Photoelectron Spectroscopy*, John Wiley & Sons, Chichester **1992**, pp 208-209 and the references therein
[12] S. Slomkowski., D. Kowalczyk, M.M. Chehimi, M. Dealamar *Colloids and Polymer Science* **2000**, *278*, 878
[13] T.L. Barr, S. Seal, K. Wozniak, J. Klinowski *J Chem Soc, Faraday Trans* **1997**, *93*, 181
[14] R.L. Opila, J.D. Legrange, J.L. Markham, G. Heyer, C.M. Schroeder *J. Adhesion Sci. Technology* **1997**, *11*, 1
[15] R. Häßler, H. Kleinert, U. Bemmann, *Adhäsion kleben & dichten* **1997**, *41* , 41
[16] R. Häßler, K. Mai, *Adhäsion kleben & dichten* **1998**, *42*, 24
[17] R. Häßler, *Adhäsion kleben & dichten* **1999**, *43*, 30
[18] R. Häßler, E. zur Mühlen, *FARBE & LACK* **1999**, *105*, 73
[19] R. Häßler, I. Jansen, H. Kleinert, *Adhäsion kleben & dichten* **2000**, *42*, 24